Food Hydrocolloids 144 (2023) 109053

Contents lists available at ScienceDirect

Food Hydrocolloids

journal homepage: www.elsevier.com/locate/foodhyd

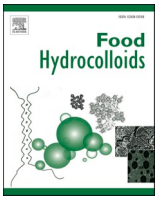

Continuous counter-current electrophoretic separation of oleosomes and proteins from oilseeds

Kübra Ayan [a], Ketan Ganar [b], Siddharth Deshpande [b], Remko M. Boom [c], Constantinos V. Nikiforidis [d,1,*]

[a] Food Process Engineering Group & Biobased Chemistry and Technology Group, Wageningen University, 6708 WG, Wageningen, the Netherlands
[b] Physical Chemistry and Soft Matter Group, Wageningen University, 6708 WG, Wageningen, the Netherlands
[c] Food Process Engineering Group, Wageningen University, 6708 WG, Wageningen, the Netherlands
[d] Biobased Chemistry and Technology Group, Wageningen University, 6708 WG, Wageningen, the Netherlands

ARTICLE INFO

Keywords:
Rapeseed
Plant proteins
Oleosomes
Sustainable separation
Electrophoresis

ABSTRACT

Oilseeds, with their high content of oil and protein, will play an important role in the transition to plant based foods. Currently, seed oil extraction involves elevated temperatures and the use of organic solvents, which degrade the quality of both oils and proteins. To take full advantage of the oilseeds, a gentler process is needed. We here propose a mild alkaline extraction followed by a continuous electrophoretic separation process that is based on differences in electrophoretic mobility and recovers intact oleosomes and proteins from the seeds. Rapeseed oleosomes and proteins are both negatively charged at pH $\geq$ 5, yet exhibit significantly different electrophoretic mobility. Therefore, separation can be achieved by imposing a counter-current hydrodynamic flow rate between their electrophoresis rate. Thus, the compounds with higher mobility, oleosomes, are retained by the electric field, and the compounds with lower mobility, proteins, go along with the flow. The separation was modeled using the Nernst-Planck equation and demonstrated using a PDMS-based microfluidic system. Both the modeling and the experimental studies confirmed that the direction and rate of migration of the compounds can be steered by the electric field strength and the convective flow velocity. The proposed electrophoretic approach is feasible and scaleable, and may be a novel path to separate differently charged components under mild conditions, thereby preserving their original native properties.

1. Introduction

Oilseeds are valuable crops with an annual production rate exceeding 600 MT (USDA, 2022; Zhou et al., 2020). The current practices in oil extraction hinder the complete use of the oilseeds as they cause irreversible changes in the structure of both natural oil-storing organelles (oleosomes) and the remaining proteins, due to the combination of the use of organic solvents and high temperature (hot pressing and desolventizing) during the process (Fetzer et al., 2020; Ntone et al., 2020; Salazar-Villanea et al., 2016). In fact, intact oleosomes are highly stable natural oil-in-water vesicles that store triacylglycerols (TAGs) in a phospholipid–protein protective monolayer and can replace man-made emulsions used in food systems (Nikiforidis, 2019). Undenatured oilseed proteins exhibit comparable functionalities as animal proteins, such as foaming and emulsifying, which are important to create desired food structures (Tan et al., 2011). To recover intact oleosomes and undenatured proteins from oilseeds, a novel approach must be devised that avoids the use of adverse processing conditions.

As an alternative to conventional oil extraction, milder fractionation processes have been suggested, in which water is used as an extraction medium to simultaneously extract intact oleosomes and proteins (Ntone et al., 2020; Berghout et al., 2014; Nikiforidis & Kiosseoglou, 2009). The obtained extract is a mixture of oleosomes and proteins, which are then separated through a centrifugation step to collect oleosome-rich (light) and protein-rich (heavy) fractions. However, this centrifugation step is capital intensive, and requires significant maintenance and copious amounts of water when applied on industrial scales (Najjar & Abu-Shamleh, 2020; Romero-Guzmán, Jung, et al., 2020; Rosenthal

* Corresponding author. Biobased Chemistry and Technology Group, Wageningen University, 6708 WG Wageningen, the Netherlands.
E-mail addresses: kubra.ayan@wur.nl (K. Ayan), ketan.ganar@wur.nl (K. Ganar), siddharth.deshpande@wur.nl (S. Deshpande), remko.boom@wur.nl (R.M. Boom), costas.nikiforidis@wur.nl (C.V. Nikiforidis).
[1] Visiting address: Building Axis-Z, no. 118, Z1102, Bornse Wellanden 9, 6708WG, Wageningen, The Netherlands.

https://doi.org/10.1016/j.foodhyd.2023.109053
Received 13 March 2023; Received in revised form 3 July 2023; Accepted 5 July 2023
Available online 8 July 2023

et al., 1996; Torres-Acosta et al., 2019).

In this work, we report on the fractionation of oleosomes and proteins with steady-state, counter-current electrophoresis. Using an electrical driving force has the advantages that (i) it is an efficient and selective driving force by acting only on individual charged particles instead of the complete suspension (Buszewski et al., 2013; Manouchehri et al., 2000), and (ii) it provides an opportunity to develop a continuous separation process when combined with a pressure-driven flow (PDF). In our case, the separation is accomplished as a net result of electrophoresis and a counter-current PDF. When the PDF velocity is set between the electrophoresis rates of the components to be separated, those with higher electrophoretic mobility are retained by the electric field, while the lower-mobility particles are taken up by the PDF (Kenyon et al., 2012; Meighan et al., 2009).

As a model system, we used rapeseed oleosomes and rapeseed storage proteins, cruciferins (12S globulins) and napins (2S albumins). Cruciferins are hexamers with a molecular weight ranging between 230 and 300 kDa and an estimated radius of 4.4 nm. On the other hand, napins are monomeric proteins with molecular weight of 12–17 kDa and an estimated radius is 1.7 nm (Ntone et al., 2021; Östbring et al., 2020). The separation principle is demonstrated with a simple mathematical model using the Nernst – Planck equation that predicts the concentration change of a compound under the influence of diffusion, electrophoresis, and convection (PDF). The properties of the components are characterized, and microfluidic devices are then used to experimentally demonstrate the feasibility of the principle. We conclude with an outlook towards upscaling the principle to larger scales.

2. Theory

The proposed system employs an electric field over a porous barrier, which is required to guarantee a homogeneous flow rate. We assume that the pores in the barrier are cylindrical and parallel to the electric field. At the same time, a counter – acting PDF is imposed. If the magnitude of the PDF velocity is adjusted in between the electrophoretic migration rate of two compounds, the compound with a lower electrophoresis rate will pass through the channel with the flow, while the other compound with a higher electrophoresis rate will be retained by the electric field. The electrophoresis rate (v_E) is equal to the product of the electrophoretic mobility (μ, μmcm/Vs equivalent to 10^{-8} m^2/Vs) and the applied electric field strength (E, V/cm) (Equation (1)).

$$v_{E,i} = \mu_i \bullet E \qquad \text{Equation (1)}$$

Fig. 1 illustrates the separation of two negatively charged particles (Particle 1 and 2) in the case of $\mu_1 > \mu_2$. The principle can be understood with the Nernst-Planck equation (Equation (2)) that describes the transport of compounds resulting from the combined effects of convective flow (PDF), an electric field, and diffusion arising from a concentration gradient (Moshtarikhah et al., 2017). We assume that sufficient electrolytes are present and that the effects of ionic interactions between the compounds can be neglected. Further nonidealities in the system are neglected as well.

$$N_i = -D_i\frac{dC_i}{dx} - D_i\frac{C_i z_i F}{RT}\frac{d\Phi}{dx} + c_i v \qquad \text{Equation (2)}$$

Here, N_i is the mass flux (kg/m^2·s) of component i, D_i is the diffusion coefficient of the component i, C_i is the concentration (kg/m^3) of the component i, x is the channel length (m), z_i is the charge number of the component i, F is Faraday's constant, R is the universal gas constant, T is the absolute temperature (K), Φ is the electric potential (V) and v is the flow velocity (m/s). In Equation (2), diffusive, electrophoretic, and convective contributions are represented by the terms of $-D_i\frac{dC_i}{dx}$, $-D_i\frac{C_i z_i F}{RT}\frac{d\Phi}{dx}$ and $c_i v$, respectively.

Equation (2) can be simplified by noticing that the term of $-D_i\frac{z_i F}{RT}\frac{d\Phi}{dx}$ is the driving force that induces an electrophoretic migration of the component i ($v_{E,i}$), and we can use an overall mass balance as a boundary condition, given that N_i must be equal to the product of the concentration at the end of the channel (C_{iL}) and the net velocity of the component i (v_i). Therefore, Equation (2) can be expressed as Equation (3);

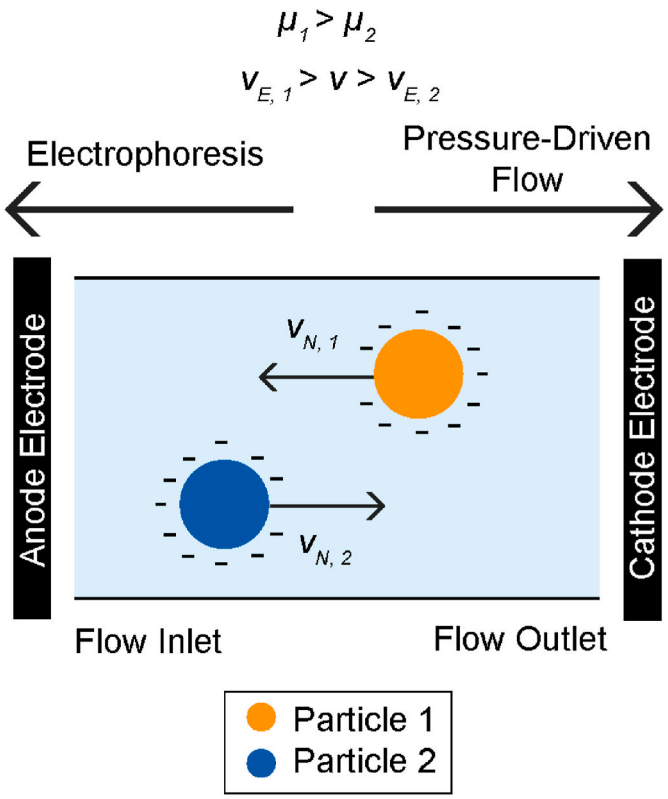

Fig. 1. Illustration of the designed electrophoretic separation system in case of negatively charged particles exhibited different electrophoretic mobility. μ: Electrophoretic mobility, v_E: Electrophoresis rate, v: Pressure driven flow velocity, v_N: Sum of v_E and v.

$$C_{iL}v_i = -D_i\frac{dC_i}{dx} + C_i\left(v_{E,i} + v\right) \qquad \text{Equation (3)}$$

This inhomogeneous ordinary differential equation can be solved using two boundary conditions. The first boundary condition is the concentration of the component i is equal to its initial concentration ($C_i = C_{i0}$) at x = 0 (inlet of the separation channel), and the second one is the flux at x = L (outlet of the separation channel) is equal to product of the final concentration of the component i and the flow velocity ($N_i = C_{iL}v$) as the component i is captured by the solvent flow at the end of the channel. When Equation (3) is solved using these boundary conditions, the following relation (Equation (4)) between the initial and the final concentration of the component i is obtained;

$$\frac{C_{iL}}{C_{i0}} = \frac{v_{E,i} + v}{v + v_{E,i}e^{\frac{-x\left(v+v_{E,i}\right)}{D_i}}} \qquad \text{Equation (4)}$$

Equation (4) gives us the concentration of the component i over the separation channel. The relation can be simplified by considering that the exponential term is very large when $v + v_{E,i} \ll 0$, and therefore the concentration of the component i on the downstream side will be very low. If $v + v_{E,i} \gg 0$, then the exponential term is very small and can be neglected. Therefore, Equation (4) might be approximated by Equation (5);

$$\frac{C_{iL}}{C_{i0}} = \begin{cases} 0 & \text{when } v + v_{E,i} < 0 \\ \dfrac{v + v_{E,i}}{v} & \text{when } v + v_{E,i} > 0 \end{cases} \quad \text{Equation (5)}$$

As Equations (4) and (5) show, the separation is dominated by the relation between v and $v_{E,i}$, and C_{iL} can be predicted from the ratio of $v/v_{E,i}$. When the value of v is larger (in absolute value) than $v_{E,i}$, the component i should pass the channels, but if v is smaller than $v_{E,i}$, then the component i should be retained by the electric field. Fig. 2 shows the typical concentrations obtained for components with different $v_{E,i}$ values at the channel outlet predicted by both Equation (4) and Equation (5). Fig. 2 indicates that Equation (5) provides a good approximation.

The separation of components based on their electrophoretic mobility and a counter-current flow as described in Equation (4) can be applied to the separation of oleosomes and proteins. Further insight into the degree of separation can be obtained by defining the selectivity of the separation as the ratio of the content of the proteins and the oleosomes in the outlet stream ($C_{proteins,L}$ and $C_{oleosomes,L}$) normalized with their initial concentrations ($C_{proteins,0}$ and $C_{oleosomes,0}$) (Equation (6));

$$\text{Selectivity} = \frac{C_{proteins,L}}{C_{proteins,0}} \Big/ \frac{C_{oleosomes,L}}{C_{oleosomes,0}} = \frac{C_{proteins,L}}{C_{proteins,0}} \cdot \frac{C_{oleosomes,0}}{C_{oleosomes,L}} \quad \text{Equation (6)}$$

By regarding the system in one dimension, we neglect effects from the non-uniform Poiseuille (parabolic) flow, so we assumed the PDF velocity is the same throughout the channel. The convection term ($c_i v$) in the case of continuous electrophoresis systems is a combination of the PDF and electroosmotic flow (EOF). EOF is a bulk fluid motion caused by the surface potential of channel walls (Lim & Lam, 2021), and depends, amongst others, on the ionic strength and the properties of the channel wall. For matter of simplicity, we here neglected the EOF effects as well. Any temperature changes due to joule heating could cause alterations in the solvent viscosity and the electrophoretic mobility of the compounds, but they were also neglected.

Overall, the input parameters for the modelling of the electrophoretic separation of oleosomes and proteins are v (m/s), E (V/m), D_i (m^2/s), C_{i0} (kg/m^3), μ_i (m^2/Vs) and z_i. The diffusivity D_i can be experimentally measured or estimated using Equation (7).

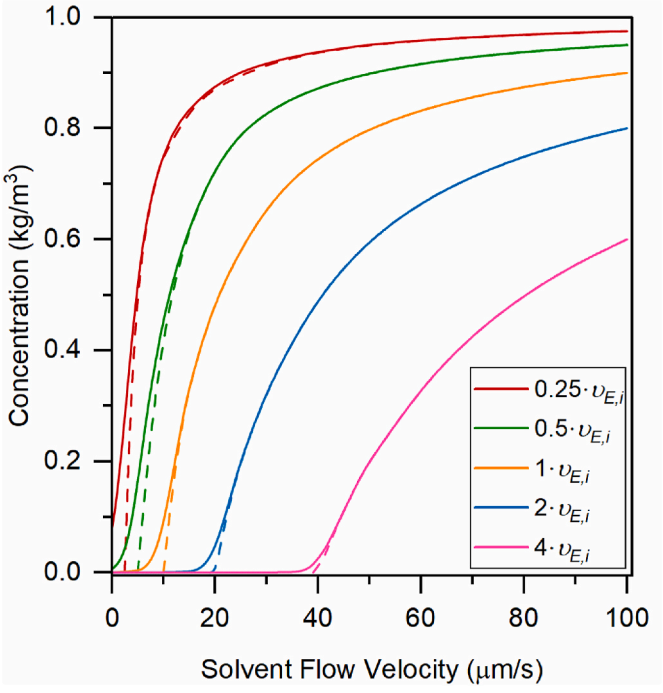

Fig. 2. Typical concentrations in the downstream side (C_{iL}) of the separation channel for different values of the electrophoretic velocities ($v_{E,i}$) predicted by Equation (4) (solid lines). The concentrations are also quite well approximated with Equation (5) (dashed lines).

$$D_i = \frac{kT}{6\pi\eta R_i} \quad \text{Equation (7)}$$

In which k is the Boltzmann constant ($1.3806 \cdot 10^{-23}$ m^2 kg/s^2·K), η is the dynamic viscosity of the medium (Pa·s) and R_i is the hydrodynamic radius (m) of component i. For relatively simple ionic components the valency, z_i, will be known; for more complex components such as oleosomes, the valency can be estimated using the electrophoretic mobility and the diffusivity (Equation (8)).

$$z_i = \frac{\mu_i RT}{D_i F} \quad \text{Equation (8)}$$

3. Materials and methods

3.1. Materials

The rapeseeds that were used for oleosome and protein extraction were of the Alizze variant (*Brassica napus*) and were kindly provided by a seed breeder. All chemicals used were analytical grade and purchased from Sigma Aldrich (St. Louis, MO, USA). Deionized water (Milli-Q, Merck Millipore, Darmstadt, Germany) was used to prepare all solutions and dispersions.

3.2. Extraction of oleosomes and proteins from rapeseeds

Oleosomes and proteins were extracted from rapeseed following the methods described by Romero-Guzmán, Vardaka, et al. (2020) and Ntone et al. (2021) with some modifications. Briefly, 100 g of rapeseeds were dispersed in deionized water at 1:8 (w/w) ratio and the pH of the dispersion was adjusted to 9.0 by adding 1.0 M NaOH. The dispersion was stirred at 400 rpm for 4 h at room temperature. Then, the dispersion was blended at 7200 rpm (Thermomix TM31, Utrecht, the Netherlands) for 90 s, and the slurry was collected. To remove much of the solids, a twin-screw press (Angel 7500, Naarden, the Netherlands) was used and the juice that contains the oleosomes and proteins was collected. The pH of the juice was re-adjusted to 9.0 by adding 1.0 M NaOH and it was centrifuged at 10000 g and 4 °C for 30 min (Sorvall Lynx 4000 Centrifuge, Thermo Scientific, USA). The centrifugation resulted in three layers: the oleosome – rich cream (top layer), a protein extract (middle part) and a fibre-rich residue (precipitant). To further purify the oleosomes, co-extracted proteins and other compounds were washed out twice by dispersing the oleosome cream in 0.1 M $NaHCO_3$ at 1:4 (w/w) ratio and centrifuged at 10000 g and 4 °C for 30 min to obtain the washed oleosome cream. To remove traces of $NaHCO_3$, the collected oleosome cream was washed once with deionized water in the same conditions. Finally, the purified oleosome cream was collected and stored at 4 °C prior to further analysis.

To isolate cruciferins and napins from the protein extract, a combination of ultrafiltration and diafiltration systems (Vivaflow 200, Sartorius, Germany) was used. Firstly, an ultrafiltration set-up with a 100 kDa MWCO PES membrane was used, and the retentate and the filtrate were collected. The retentate was dialyzed against deionized water for 72 h at 4 °C to remove any present salts, and used as a cruciferins extract. Napins and other smaller molecules (phenolics etc.) were collected in the filtrate. To remove phenolic compounds and salt, the filtrate was diafiltrated through a 5 kDa MWCO PES membrane until a transparent filtrate was obtained. The obtained retentate was used as a napins extract. Both cruciferins and napins extracts were freeze-dried (Epsilon 2-10D LSCplus, Martin Christ, Germany) and stored at −20 °C prior to further analysis.

3.3. Chemical and physical characterization of the extracted oleosomes and proteins

3.3.1. Composition analysis of the extracted oleosomes and proteins

The total oil content of the oleosomes was measured using Soxhlet extraction method (B-811 Büchi Extractor, Switzerland) using petroleum ether as a solvent. First, the oleosome cream was dried at 60 °C for 24 h and 1 g of dried oleosome cream was extracted for 3 h; then the extracted oil was collected and weighed. Equation (9) was used to calculate the total oil content on a dry basis.

$$\text{Oil Content } (wt\%) = \frac{\text{Amount of extracted oil } (g)}{\text{Amount of dry unextracted sample } (g)} * 100\% \quad \text{Equation (9)}$$

The total protein content in the defatted oleosome cream and protein isolates was measured using the Dumas method (Rapid N exceed, Elementar, Germany) using a nitrogen conversion factor of 5.7 to calculate the total protein content. For the analysis, aspartic acid was used as a standard, O_2 served as a blank sample and 100–150 mg of dried oleosome cream and protein extract were used as samples. The analysis was performed in triplicate and the results were expressed as mean ± the standard deviation.

3.3.2. Qualitative analysis of the protein profile

To analyze the proteins in the oleosome and protein extracts, Sodium Dodecyl Sulfate Polyacrylamide Gel Electrophoresis (SDS-PAGE) was used both under reducing and non-reducing conditions. Polypeptides are observed according to their overall molecular weight under non-reducing conditions, and subunits of the polypeptides are analyzed under reducing conditions by adding a reducing agent that acts on the disulfide bonds in protein complexes and cleaves them.

SDS-PAGE analysis was conducted as follows: Oleosome and protein samples were prepared to obtain a final protein concentration of 1 mg/mL and 100 μL of this sample was mixed with 250 μL of sample buffer (NuPAGE LDS, Thermo Fisher, the Netherlands). For reducing conditions, 100 μL of reducing agent (NuPAGE Sample Reducing Agent, Thermo Fisher, the Netherlands) was added. Then, the volume was topped to 1 mL by adding deionized water. All samples were first centrifuged at 2000 g for 1 min at room temperature and heated to 70 °C for 10 min. After a final centrifugation under the same conditions, the samples (20 μL) were loaded into the SDS – PAGE gel (NuPAGE Novex 4–12% Bis-Tris Gel, Thermo Fisher, the Netherlands). A protein marker (10 μL) (PageRuler™ Prestained Protein Ladder, 10–180 kDa) was used as a standard. To run the system, MES buffer (NuPAGE MES SDS Running Buffer, Thermo Fisher, the Netherlands) was added to the buffer chamber and the system was operated under 200 V for 30 min. After the electrophoresis, the gel was washed with deionized water for 20 min to remove any residues of the running buffer, and then the gel was dyed overnight with Bio-safe Coomassie Stain (Bio-Rad Laboratories B.V., the Netherlands). Following this, the gel was destained overnight by deionized water. The obtained bands were analyzed using a gel scanner (GS900 Gel Scanner, Bio-Rad Laboratories B.V., the Netherlands).

3.3.3. Particle size measurement

The droplet size distribution of the oleosomes was determined using static laser light diffraction (Mastersizer 3000, Malvern Instruments Ltd, UK). The oleosome cream was diluted in deionized water to a concentration of 1.0 wt% for the measurement. The refractive index of the oleosome cream was assumed to be 1.47 and that of water (dispersion phase) to be 1.33. The mean particle size was obtained as a result of three replicate experiments and expressed by both the surface ($d_{3,2}$) and the volume ($d_{4,3}$) weighed mean diameter ± standard deviation (μm). Besides, the particle size distribution was given as volume density.

To determine the particle size of the protein extracts (cruciferins and napins), dynamic light scattering (ZetaSizer Ultra, Malvern, UK) was used. Protein solutions of 0.001 wt% concentrations were prepared at different pH values (2.0–12.0) and all samples were stirred at 200 rpm for 4 h at room temperature prior to the measurement. The particle size distribution was obtained as a result of three replicate experiments, and the particle size was expressed as the intensity-based mean diameter ± standard deviation (nm). The particle size distributions were given as intensity (%).

3.3.4. ζ-Potential measurement

The ζ-potentials of the oleosomes and protein extracts were measured using electrophoretic light scattering (ELS) (ZetaSizer Ultra, Malvern, UK). The electrophoretic mobilities were collected from the same measurements using the following relation (Equation (10)).

$$\mu = \frac{2\varepsilon\zeta f(\kappa\alpha)}{3\eta} \quad \text{Equation (10)}$$

In which ε is the dielectric constant, $f(\kappa\alpha)$ is Henry's function and η is the viscosity of the suspending medium. To measure the ζ-potential, 0.01 wt % of oleosome suspension or protein solution was prepared using deionized water and the pH of the solutions was adjusted between 2.0 and 12.0 using 0.1 M NaOH and 0.1 M HCl. Then, the samples were stirred at 200 rpm for 2 h and the ζ-potential was measured at 25 °C by applying 220 V potential difference. For the refractive indices, 1.47 and 1.59 were used for the oleosomes and the proteins, respectively, and 1.33 was used for the dispersant (water). The same measurement was done using 1.0 mM potassium phosphate buffer at pH 8.0 as a dispersant. The measurements were done in triplicate using a fresh sample each time to eliminate any detrimental effect of the electric field on particles, like aggregation. The results were converted into electrophoretic mobility and given as average ± standard deviation (μmcm/Vs).

3.4. Fabrication of the microfluidic device for the demonstration of the electrophoretic separation

A PDMS-based microfluidic device was fabricated to serve as a micro-scale separation channel that would allow direct observation of the particle movement using a fluorescence microscope. First, a silicon wafer including the channel design was prepared using soft lithography. In brief, a silicon wafer (76 mm in diameter) was coated with SU-8 25 photoresist (Kayaku, MA, USA) to obtain 30 μm final thickness using a two-step spin coating (500 rpm for 30 s and 1800 rpm for 45 s). Then, the wafer was soft-baked overnight at 65 °C and cooled down to room temperature for 15 min. Next, the design was printed on the wafer, using a micro-writer device (MicroWriter ML3, Durham Magneto Optics Ltd., Germany) with the exposure energy adjusted to 350 mJ/cm^2. The wafer was then post-baked at 65 °C for 2 min, followed by 95 °C for 10 min and cooled down to room temperature. To remove the excess uncured photoresist, the wafer was first washed with propylene glycol monomethyl ether acetate (PGMEA), followed by deionized water. To ensure strong adhesion of the printed pattern to the surface, the wafer was baked at 120 °C for 20 min. Finally, the unprinted side of the wafer was glued to a petri dish to be used as a mold for microfluidic chip fabrication.

To make PDMS devices, PDMS and a curing agent (SYLGARD™ 184 Silicone Elastomer) were mixed at a 10:1 (w/w) ratio for 15 min under continuous rotation at 60° and 20 rpm. Since the mixing process traps air bubbles, a short centrifugation step at 100 rpm for 2 min at room temperature was carried out to remove the trapped air. The prepared PDMS mixture was poured onto the printed mold wafer, placed in a vacuum chamber, and degassed. After removing all air bubbles, the wafer with the PDMS was baked at 70 °C for 4 h. To obtain a homogenous surface in the channels, glass slides were coated with PDMS. For this purpose, PDMS (approximately 1–2 g) was added at the center of the glass slide and spread by spinning at 500 rpm for 30 s and 3000 rpm for 15 s using a

spin coater. Similar to the above-mentioned PDMS curing, the glass slides were also baked at 70 °C for 4 h. The cured PDMS was peeled off from the wafer, and individual channels were cut out from the whole PDMS layer. Two 0.75 mm holes to serve as inlet and outlet were punched on the channels using a biopsy punch. To perform an EOF measurement, 5 mm holes were punched instead of 0.75 mm to serve as reservoirs for the buffer solution. To make a closed channel, PDMS-coated glass slides and the PDMS block with channels were covalently bonded using plasma for 15 s (Plasma Cleaner PDC–32 G, Harrick Plasma, NY, USA). After 3 h, the channels were coated with 5% w/v polyvinyl alcohol (PVA) solution for 2 min to render the surface of the PDMS hydrophilic. Excess free PVA was removed by flushing the channel with nitrogen gas. Lastly, the channels were baked at 120 °C for 40 min to fixate the PVA coating. The dimensions of an individual channel were 2 cm in length, 400 μm in width, and 30 μm in depth.

3.5. Electroosmotic flow measurement

As aforementioned, EOF is the flow of an electrolyte solution under the influence of an electric field due to the surface charge of the channel walls. To estimate the magnitude of the EOF in the fabricated PDMS channels, the current-monitoring method described by Saucedo-espinosa and Lapizco-encinas (2016) was used with some further modifications. This method measures the changes in the current value as a result of the exchange of electrolyte solutions that differ slightly in their ionic concentration due to EOF. Initially, the inlet reservoir and the channel were filled with low ionic concentration electrolyte solution (9.0 mM potassium phosphate buffer) and the outlet reservoir was filled with a higher ionic concentration electrolyte solution (10.0 mM potassium phosphate buffer). A stainless-steel wire was dipped into each reservoir and connected to a high-voltage power supplier (HCN 140–20000, Fug, Germany). When a potential difference of 600 V was applied, the current value started to increase as the lower-concentration electrolyte solution started to replace the higher-concentration electrolyte solution, and the overall conductivity in the channel increased. A stationary value indicated that the original electrolyte solution in the channel had been completely replaced. During the experiment, the current value was recorded over time and the total time to reach the plateau value was determined. The EOF velocity (v_{EOF}) was calculated by dividing the channel length (L) by the duration of the solution exchange (Δt) (Equation (11)). The ratio of v_{EOF} to E gives the EOF mobility (μ_{EOF}) (Equation (12)). The measurements were performed in triplicate and the result was given as average EOF mobility ± standard deviation (μmcm/Vs).

$$v_{EOF}(\mu m / s) = \frac{L\ (\mu m)}{\Delta t\ (s)} \qquad \text{Equation (11)}$$

$$\mu_{EOF}(\mu mcm / Vs) = \frac{v_{EOF}\ (\mu m/s)}{E\ (V/cm)} \qquad \text{Equation (12)}$$

3.6. Electrophoretic separation of the extracted oleosomes and proteins

To investigate the particle movement under the combined influence of the electrophoresis and the PDF, a microfluidic experimental setup was used. The setup includes an inverted fluorescent microscope (Nikon-Ti2-Eclipse), a pressure pump (OB1 MK3+, Elveflow, France), and a power supply. The oleosomes and the proteins were stained by curcumin ($\lambda_{ex} = 430$ nm) and fast green dye ($\lambda_{ex} = 633$ nm) at a ratio of 100:1 (v/v), respectively. The samples were visualized using a pE-300^{ultra} illumination system and a Nikon 20 x/0.75 NA air objective. All the samples were illuminated at 1–5% laser intensity and time-lapse images were acquired using a Prime BSI Express CMOS camera at an exposure time of 30 ms.

For the demonstration of the separation principle, we used 1.0 mM potassium phosphate buffer at pH 8.0 to eliminate pH fluctuations due to the electrolysis of water to some extent and the experiment duration was limited to 20 s to make sure the pH of the medium remained constant during the analysis. First of all, the samples of oleosomes and proteins were prepared at a concentration of 0.01 wt% in the buffer. Then, the sample was introduced into the micro-channel using the pressure pump connected to PDMS channel with 0.5 mm ID silicone tubing and 25 μm ID flow resistor tubing. Two metal fittings were attached to the channel inlet and outlet to serve as electrodes. Both metal fittings were connected to the power supply using crocodile clips. Once the channel was filled with the sample, the flow velocity and potential difference were adjusted to the desired values.

Before the experiment, the oleosomes and the proteins were analyzed under (i) constant pressure (50 mBar) and a stepwise increase of electric field (0–100 V/cm) and (ii) constant electric field (50 V/cm) and a stepwise increase of pressure (0–200 mBar) to reveal the movement direction and net velocity of the particles under specific conditions. The combination of the electric field and the pressure difference that caused the oleosomes and the proteins to move in opposite directions was used for the separation experiment. The movement of the particles was recorded at a rate of 1 frame per second (fps) for each experiment, and the recordings were further analyzed using the particle tracking module in ImageJ software to measure the particle velocities (Schneider et al., 2012). Particles that move near the walls were neglected to eliminate the effects of a parabolic flow profile, so only the particles at or near the center of the channel were tracked.

3.7. Statistical analysis

The electrophoretic mobility measurements were performed in triplicates. Statistical analysis was carried out by using SPSS version 25.0 for Windows (IBM Corp. NY, USA) to identify significant differences in the electrophoretic mobility of the oleosomes and the proteins at various pH values. For this purpose, one-way ANOVA and the Tukey test were used. Significance of the differences was assessed based on the 95% confidence limit ($P < 0.05$).

4. Results and discussion

4.1. Characterization of the extracted oleosomes and proteins

After the extraction of the rapeseed oleosomes and proteins (cruciferins and napins), their composition and physicochemical properties were determined.

The composition of the oleosome cream was 92.24 ± 5.93 wt% oil and 2.59 ± 0.02 wt% proteins on a dry basis, and protein contents of the extracted cruciferins and napins were 79.19 ± 0.31 wt% and 85.25 ± 0.17 wt% on a dry basis, respectively. SDS-PAGE analysis showed that the oleosome extract was free from any co-extracted rapeseed storage proteins and was dominated by membrane-bound proteins, oleosins (Figure S-1, see Supplementary Information). The profiles of the protein extracts indicated that the napin isolate was free of cruciferins, however, the cruciferin isolate also included some napins (Figure S-1).

The size distribution of the extracted oleosomes at neutral pH is presented in Fig. 3A. The distribution is bimodal with two peaks at around 0.6 and 5.0 μm ($d_{3,2}$: 1.18 ± 0.26 μm and $d_{4,3}$: 2.76 ± 0.94 μm). The bimodality indicates that some individual oleosomes formed aggregates, probably as a result of flocculation and/or coalescence due to electrostatic and hydrophobic attractive forces (Romero-Guzmán, Petris, et al., 2020). Similar observations have been previously reported, where besides individual oleosomes with a diameter of around 1 μm, oleosome aggregates were present as well (diameter >2.5 μm) (Romero-Guzmán, Köllmann, et al., 2020; De Chirico et al., 2018).

The size distributions of the proteins at pH 8.0 are shown in Fig. 3B. Both size distributions are bimodal as well. In the case of cruciferins, both peaks (~200 and 1200 nm) are far above their reported native size of 8.8 nm which shows the presence of larger cruciferin clusters. The

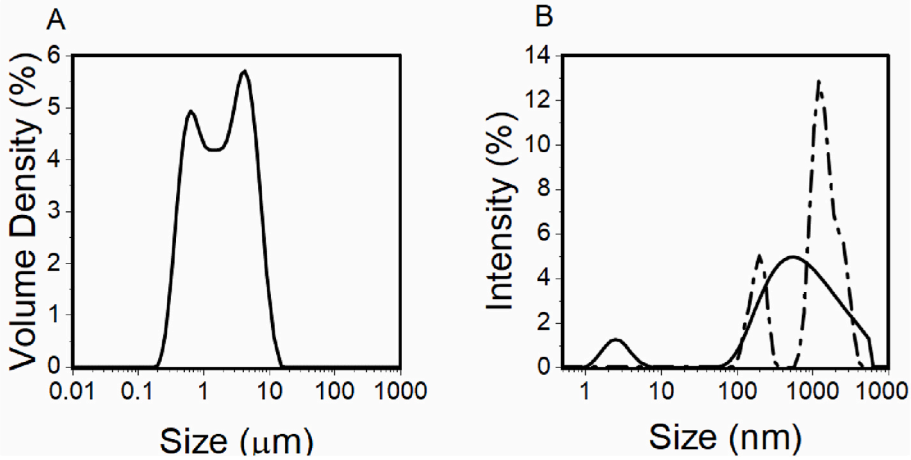

Fig. 3. A) Size distribution of the extracted oleosomes at pH 7.0 B) Size distribution of the extracted cruciferins (dashed line) and napins (solid line) at pH 8.0.

napins extract showed two peaks at around 3 nm and 600 nm which implies the presence of both native napins (3.4 nm) and napin aggregates. The protein aggregation might have been induced by the extraction/purification conditions, like agitation speed, pH, pressure and freeze drying (Callahan et al., 2014; Li et al., 2020; Mahler et al., 2009). In a practical sense, the formation of larger protein particles makes the observation of the proteins under a fluorescent microscope much easier, but one has to bear in mind that these aggregates may have different mobility than molecularly dissolved proteins.

To evaluate the suitability of the proposed electrophoretic separation system for rapeseed oleosomes and proteins, their electrophoretic mobilities were measured at pH values from 2.0 to 12.0, as shown in Fig. 4. Both the oleosomes and the proteins have very close isoelectric points, between pH values of 5.0 and 6.0, where the particles carry zero net charge, so both are charged either positively or negatively at any pH. This means that they should move in the same direction under the influence of only an electric field. However, the electrophoretic mobility of the oleosomes is much greater than that of the proteins at pH $\geq$ 5.0 ($P < 0.05$). The largest difference was 3.61 μmcm/Vs at pH 11.0, but the difference remains in the same range between pH 7.0 and 12.0. The larger mobility of the oleosomes may be because of their higher surface charge than proteins, but may also arise from the fact that larger particles, like oleosomes, exhibit lower hydrodynamic frictional forces relative to their volume (van Oss, 1975).

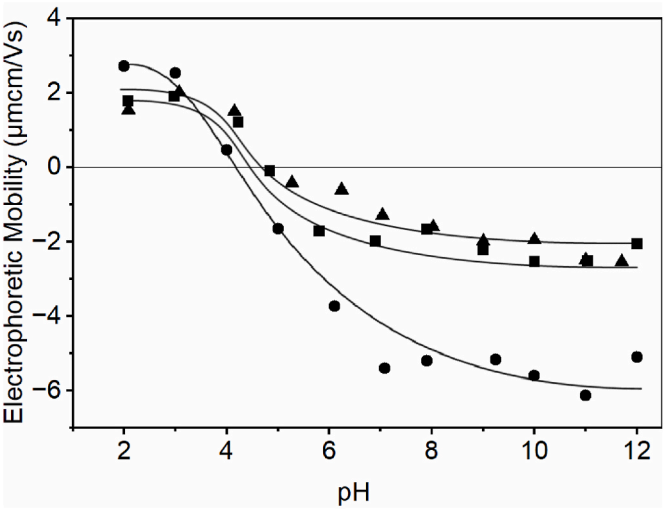

Fig. 4. Electrophoretic mobility of oleosomes (●), cruciferins (■) and napins (▲) at pH 2.0–12.0. Solid lines are guide for the eyes.

The results indicate that the oleosomes and the proteins can be separated using the electrophoretic separation system. For example, at pH 8.0 with a 10 V/cm electric field and a 30 μm/s counter–current flow velocity, the oleosomes will move under the influence of the electric field with a net velocity of −21.9 μm/s, while the proteins have a net velocity of +13.7 μm/s and are dragged along by the solvent flow.

For the experimental demonstration, pH 8.0 was selected since it provides a significant difference in the electrophoretic mobility and is still a mild pH. A buffer system was used to minimize the effects of electrolytic reactions during the experiment. The electrophoretic mobilities of the extracted oleosomes, cruciferins and napins in 1.0 mM potassium phosphate buffer were determined as −3.205 ± 0.136, −1.942 ± 0.169 and −1.266 ± 0.211 μmcm/Vs, respectively. The electrophoretic mobility of the oleosomes was 1.5-fold lower than when dispersed in the buffer. The main reason for this is the increasing ionic strength screening the surface charges (Semenov et al., 2010).

4.2. Interpretation of the experimental parameter values

The electrophoretic mobility measurements revealed that the oleosomes and the proteins have different electrophoretic mobilities at most pH values, which indicates that their electrophoretic separation is achievable. This can be further quantified by using the Nernst – Planck equation (Equation (4)). Table 1 shows the data used and Fig. 5 summarizes the findings.

In Table 1, z_i values of the proteins are given not for an individual protein molecule but for larger protein clusters, which probably formed during the extraction process.

In the proposed separation system, the components with low electrophoresis rate relative to the PDF velocity, are expected to flow toward the downstream side, which can be called a permeate. The original feed will become enriched in components with a high electrophoresis rate relative to the PDF velocity, and exit the system as a retentate. The former category will comprise the proteins, while the oleosomes accumulate in the retentate. To be successful, the separation requires the

Table 1
Electrophoretic mobility, particle size, charge number and diffusion coefficient values for oleosomes, cruciferins and napins at pH 8.0 and 1.0 mM potassium phosphate buffer.

Compound	Electrophoretic Mobility ($m^2/V{\cdot}s$)	Radius (m)	Charge Number (z_i)	Diffusion Coefficient (D_i) (m^2/s)
Oleosomes	$-3.205{\cdot}10^{-8}$	$1.38{\cdot}10^{-6}$	−5203.55	$1.58{\cdot}10^{-13}$
Cruciferins	$-1.942{\cdot}10^{-8}$	$7.60{\cdot}10^{-7}$	−1735.28	$2.87{\cdot}10^{-13}$
Napins	$-1.266{\cdot}10^{-8}$	$1.84{\cdot}10^{-7}$	−273.69	$1.19{\cdot}10^{-12}$

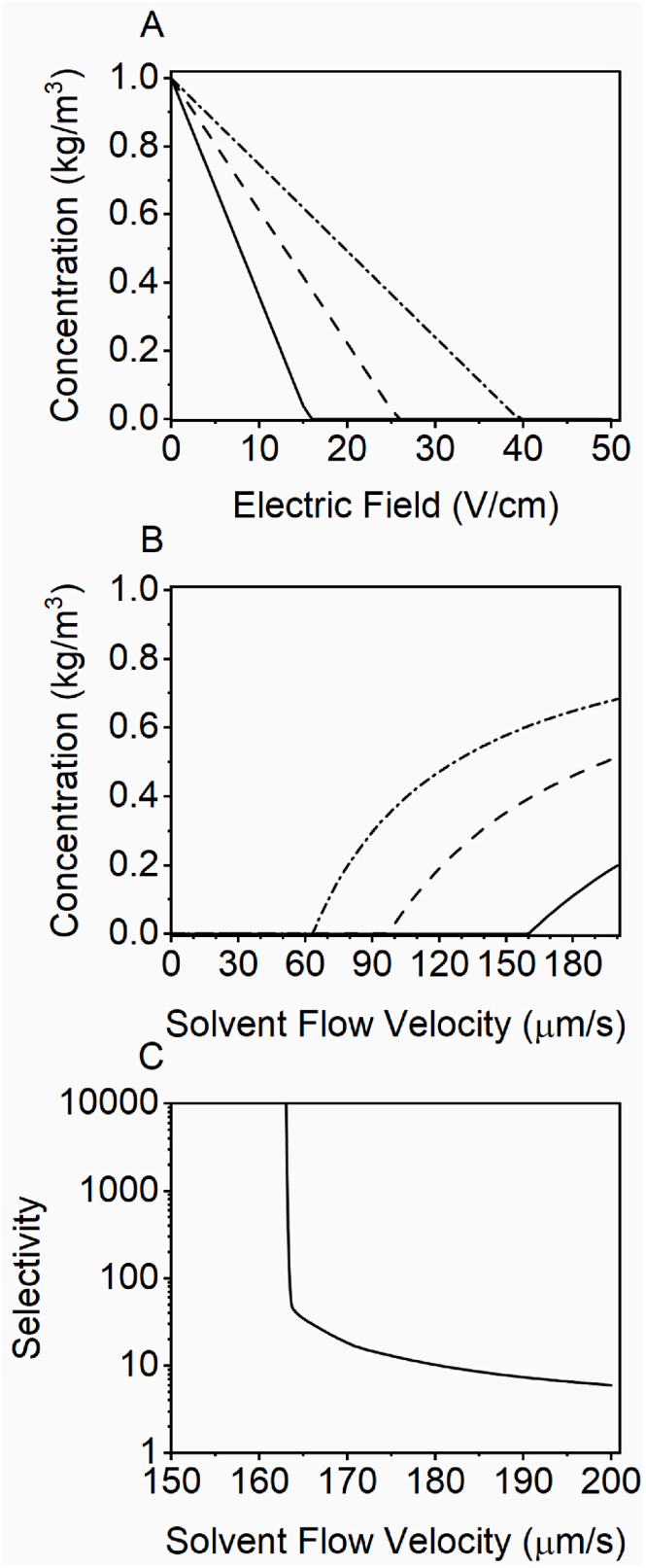

Fig. 5. Predicted concentrations of oleosomes (—), cruciferins (- -) and napins (-•-) in the permeate under A) increasing electric field and 50 μm/s constant solvent flow velocity, and B) increasing solvent flow velocity and 50 V/cm constant electric field. C) Selectivity of the separation under increasing solvent flow velocity and 50 V/cm constant electric field.

right balance between the applied electric field and the convective flow applied.

We can now combine the model with the values of the electrophoretic mobilities that we measured. If we assume a channel length of $L = 100\ \mu m$ and a PDF velocity of $v = 50\ \mu m/s$, introducing the electric field leads to a reduction of the concentration of the oleosomes and the proteins in the permeate. Fig. 5A shows the effect of increasing the electric field on the outlet concentrations of the oleosomes and the proteins. Their full retention starts at different values of the electric field strength. The oleosomes, having higher electrophoretic mobility, are the first compounds completely retained by the electric field at 16 V/cm. Thus, separation between the oleosomes and the proteins is achieved as both cruciferins and napins are still in the permeate. However, an increase of the electric field to 27 V/cm results in the full retention of both oleosomes and cruciferins, with only napins present in the permeate. An even further increase of the electric field to 46 V/cm results in a full retention of both oleosomes and proteins. In the last case, electrophoresis dominates the hydrodynamic flow, and no separation results.

Similarly, if we set the electric field at 50 V/cm and vary the convective flow velocity, we achieve full retention of the components at low flow rates, and a breakthrough at different flow rates, depending on the individual electrophoretic migration rates of the components. Fig. 5B shows that a flow velocity exceeding 100 μm/s initiates the separation as only the proteins are present in the permeate. To drag the oleosomes to the outlet, at least 160 μm/s solvent flow is needed. Therefore, a flow velocity between 100 and 160 μm/s ensures the separation at 50 V/cm electric field. A further increase in the flow velocity, however, blocks the separation since the electric field leads to accumulation of the oleosomes together with the proteins in the permeate. This effect is escalated at even larger flow rates. Therefore, the correct balance between the PDF and the electric field is required.

The relation between oleosome – protein separation selectivity and the solvent flow velocity can be seen in Fig. 5C. At a lower flow rate the selectivity is very large, but the concentrations passing through to the permeate are also vanishingly small. A selectivity value approaching infinity indicates the concentration of oleosomes in the outlet stream is zero. This can be seen around 160 μm/s flow rate. An increasing solvent flow velocity decreases the selectivity, and a mixture of the oleosomes and the proteins is then collected in the downstream.

Overall, the analysis illustrates that the continuous electrophoretic separation system can indeed lead to the separation of rapeseed oleosomes and proteins.

4.3. Electrophoretic separation of the extracted oleosomes and proteins

The analysis above clearly indicated that the movement direction of the compounds is governed by the balance between the electric field strength and the flow velocity, and specific combinations of these two can drive the separation. To experimentally confirm this, we utilized a microfluidic device and observed the movement of the oleosomes and the proteins under the influence of the electric field and the PDF through a fluorescent microscope (Fig. 6A).

We first determined net velocity of the oleosomes and the proteins separately as function of the applied pressure (flow rate) and the electric field strength. The net velocity of the compounds was detected experimentally by analyzing the track of the particles in the recorded movies. The experimental results were compared to the theoretical net velocity values that are predicted by summing up electrophoresis rate, PDF velocity and EOF velocity. EOF mobility was measured as 0.35 ± 0.11 μmcm/Vs, and multiplying this with the electric field gives the EOF velocity (Equation (11)). Positive values of the velocity in Fig. 6B and C represent the direction of the PDF, and negative values represent the electrophoresis direction.

Fig. 6B shows the net velocity of the compounds under pressure differences ranging from 0 to 200 mBar (~0–160 μm/s) and a constant electric field of 50 V/cm. It can be seen that the proteins under 100 mBar

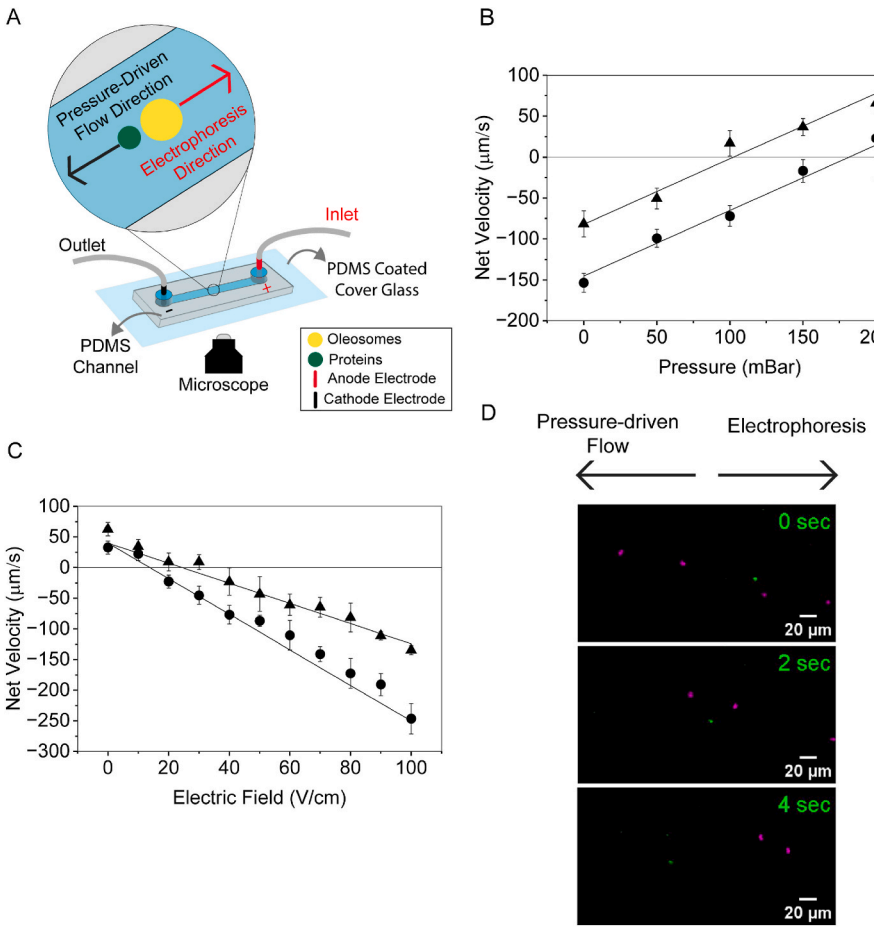

Fig. 6. A) Schematic of the experimental setup B) Net velocity of the oleosomes (●) and the proteins (▲) under increasing pressure and constant electric field of 50 V/cm and C) increasing electric field and constant pressure of 50 mBar. Lines represents the predicted net velocity taking into account electrophoresis, pressure-driven flow and electroosmotic flow. Positive and negative values represent direction of pressure-driven flow and electrophoresis, respectively. D) Movement of the oleosomes and the proteins under 120 mBar pressure and 50 V/cm electric field at time 0, 2 and 4 s. Oleosomes (magenta) and proteins (green) were visualized by curcumin (λ_{ex} = 430 nm) and fast green dye (λ_{ex} = 633 nm), respectively. Electrophoresis (right) and pressure-driven flow (left) are acting in the opposite direction.

pressure are dragged along by the solvent flow as they do not have enough electrophoretic velocity to counteract the convective flow. Under 100 mBar, the oleosomes have sufficient electrophoretic velocity to counteract the PDF and thus reverse their direction towards the electric field. This was also observed at 150 mBar pressure. Therefore, under 50 V/cm electric field, separation can be achieved between 100 and 150 mBar pressure, which results in 100–140 μm/s convective flow velocity including the EOF. The Nernst-Planck equation indicated a convective flow velocity ranging between 100 and 160 μm/s under 50 V/cm electric field ensures the separation, which is in good agreement. At a pressure of 200 mBar (total convective flow velocity: ~180 μm/s) the separation is impaired as some of the oleosomes start to get captured by the solvent flow as well.

At 200 mBar pressure, we observed unstable motion of both the oleosomes and the proteins. This may be caused by pH instabilities due to the ingression of electrolysis products, like H^+ ions, from the anode electrode into the separation channel (Agostino et al., 2014; Rudge & Monnig, 2000). The electrophoretic mobility of the oleosomes is more sensitive to pH changes than that of the proteins (Fig. 4). To avoid these complications, the pressure difference was limited to 150 mBar. In a larger – scale separator, care can be taken that no electrolysis products are added to the system, for example by using flushed electrodes. However, as the microfluidic system was only meant to demonstrate the principle, this was not implemented; nor would it have been practically feasible. Therefore, we only employed moderate electric fields, allowing separation without introducing significant pH differences.

Besides the effects of increasing convective flow velocity, a variation of the net velocity under increasing electric field strength under constant pressure of 50 mBar can be seen in Fig. 6C. Separation can be observed under an electric field value of 20–30 V/cm and a flow velocity of approximately 50 μm/s. This finding is also in good accordance with the Nernst-Planck equation, which predicted separation with an electric field of 16–27 V/cm in case of 50 μm/s convective flow velocity. The equation can therefore adequately estimate the necessary electric field strength and convective flow velocity for the separation.

The experimental demonstrations highlight that the convective flow velocity is actually a combination of PDF and EOF. The fact that EOF generally results in a stronger plug flow than pressure driven Poiseuille flow (parabolic flow profile) may make the prediction by the Nernst-Planck equation and the experimental realization better than with pure PDF. In a larger-scale separator, the EOF may be utilized to generate flow without applying pressure; otherwise, their combination should be adjusted to achieve the right convective flow velocity. In our microchannel, we experimentally set the pressure such that the right convective flow is generated. The alignment between the calculated lines and the experimental data points in Fig. 6B and C indicated this was done properly.

To directly observe the separation in the microchannel, a pressure difference of 120 mBar and an electric field strength of 50 V/cm were chosen as this combination caused the oleosomes and the proteins to move in the opposite direction with similar velocities. The separation was visualized using a fluorescent microscope and time-lapse images are presented in Fig. 6D. The directions of solvent flow and electrophoresis are to the left (cathode electrode) and to the right (anode electrode), respectively. The initial positions of the compounds are shown at t = 0 s, and the changing positions are given at the 2nd and 4th seconds. Fig. 6D shows the oleosomes moving in the direction of electrophoresis and the proteins moving in the direction of convective flow. During the separation, the net velocity of the oleosomes was detected as -37.29 ± 5.29 μm/s, and the net velocity of the single protein particle was 22.99 μm/s.

Overall, we proposed a new mechanism for separation of rapeseed oleosomes and proteins with a relatively simple model and could microscopically observe the separation itself using a microfluidic channel. We expect that the principle can be scaled up to larger processes by using a larger array of channels, for instance using a porous barrier. In an upscaled version, electrodes can be positioned on both sides of the porous medium to form an electric field. And, a convective flow can be introduced either using the pressure difference between the sides of the porous barrier or taking advantage of the electroosmotic flow. Given this approach, the electrophoretic separation system can be upgraded by utilizing electrochemical cells or electrodialysis systems. By retaining the balance between the electric field and the PDF, but increasing their absolute values, one can improve the specific throughput of the system. An important practical issue is the formation of a pH gradient between the anode and cathode electrodes due to electrolysis, which may alter the movement of the oleosomes and proteins. In our microfluidic experiment, we maintained the pH by limiting the recording time to 20 s. Over this short time, the electrolysis products have not yet reached the location of observation. In a larger system, one will have to mitigate the effects, for example by using flushed electrodes, as is often used in electrodialysis.

In practice, the electrophoretic separation system was proposed as an alternative to the centrifuge-based final separation for mild alkaline extraction products of rapeseed. This study utilized purified oleosomes and proteins to demonstrate the separation principle. However, in a real case, multiple compounds, like carbohydrates and phenolics, are present, and a multi-stage separation would be required to recover oleosomes and proteins. To perform the separation with real-life systems, the electrophoretic mobility of each species must be determined. Besides, further investigation is also needed to understand the interactions between oleosomes and proteins or other extracts at varying concentrations.

5. Conclusions

We demonstrated the principle of separating components with different electrophoretic mobilities in a steady state system by using an electric field antiparallel to the convective flow, creating a counter-current system. This can be best achieved in flow channels or with a porous barrier on larger scales, effectively providing a very large number of channels. The principle was introduced and demonstrated using a simple model based on the Nernst-Planck equation, which shows that separation can be obtained when the convective flow is in between the electrophoretic migration rates of the components to be separated. Measurements of the electrophoretic mobilities of rapeseed oleosomes and proteins revealed that the separation should indeed be possible. The separation was then confirmed by direct observation of the migration of individual components by microscopy and using a microfluidic channel. Also in this device, the differences in electrophoretic migration rates were confirmed. Finally, the separation between the oleosomes and the proteins could be directly observed. The principle of the continuous electrophoretic separation is suitable for upscaling. The number of channels can be increased using a porous barrier containing many individual channels, which also provides higher overall productivity. Since the separation rests on the balance between the convective flow rate and the applied electric field strength through the channel, increasing the latter will also allow for larger flow rates and hence productivity. The current work demonstrates that counter-current electrophoretic separation is possible and feasible with practically relevant systems, such as proteins and oleosomes from rapeseed.

Credit author statement

Kübra Ayan: Conceptualization, Investigation, Writing – original draft. **Ketan Ganar:** Resources (Microscopic Setup), Writing - Review & Editing. **Siddharth Deshpande:** Resources (Microscopic Setup), Writing - Review & Editing. **Remko M. Boom:** Conceptualization, Supervision, Writing - Review & Editing. **Constantinos V. Nikiforidis:** Conceptualization, Supervision, Writing - Review & Editing.

Funding

This work was sponsored by the Ministry of National Education (Turkey). Besides, Siddharth Deshpande acknowledges funding from the Dutch Research Council (grant number: OCENW.KLEIN.465).

Declaration of competing interest

The authors declare that they have no known competing financial interests or personal relationships that could have appeared to influence the work reported in this paper.

Data availability

Data will be made available on request.

Appendix A. Supplementary data

Supplementary data to this article can be found online at https://doi.org/10.1016/j.foodhyd.2023.109053.

References

Agostino, F. J., Cherney, L. T., Kanoatov, M., & Krylov, S. N. (2014). Reducing pH gradients in free-flow electrophoresis. *Analytical Chemistry, 86*(12), 5656–5660. https://doi.org/10.1021/ac501081b

Berghout, J. A. M., Boom, R. M., & Van Der Goot, A. J. (2014). The potential of aqueous fractionation of lupin seeds for high-protein foods. *Food Chemistry, 159*, 64–70. https://doi.org/10.1016/j.foodchem.2014.02.166

Buszewski, B., Dziubakiewicz, E., & Szumski, M. (2013). Electromigration techniques theory and practice. *Springer Series in Chemical Physics, 105*. https://doi.org/10.1007/978-3-642-35043-6

Callahan, D. J., Stanley, B., & Li, Y. (2014). Control of protein particle formation during ultrafiltration/diafiltration through interfacial protection. *Journal of Pharmaceutical Sciences, 103*(3), 862–869. https://doi.org/10.1002/jps.23861

De Chirico, S., di Bari, V., Foster, T., & Gray, D. (2018). Enhancing the recovery of oilseed rape seed oil bodies (oleosomes) using bicarbonate-based soaking and grinding media. *Food Chemistry, 241*, 419–426. https://doi.org/10.1016/j.foodchem.2017.09.008

Fetzer, A., Müller, K., Schmid, M., & Eisner, P. (2020). Rapeseed proteins for technical applications: Processing, isolation, modification and functional properties – a review. *Industrial Crops and Products, 158*, 1–18. https://doi.org/10.1016/j.indcrop.2020.112986

Kenyon, S. M., Weiss, N. G., & Hayes, M. A. (2012). Using electrophoretic exclusion to manipulate small molecules and particles on a microdevice. *Electrophoresis, 33*(8), 1227–1235. https://doi.org/10.1002/elps.201100622

Li, Y., Cheng, Y., Zhang, Z., Wang, Y., Mintah, B. K., Dabbour, M., Jiang, H., He, R., & Ma, H. (2020). Modification of rapeseed protein by ultrasound-assisted pH shift treatment: Ultrasonic mode and frequency screening, changes in protein solubility and structural characteristics. *Ultrasonics Sonochemistry, 69*, 1–10. https://doi.org/10.1016/j.ultsonch.2020.105240

Lim, A. E., & Lam, Y. C. (2021). Electroosmotic flow hysteresis for fluids with dissimilar ph and ionic species. *Micromachines, 12*(9). https://doi.org/10.3390/mi12091031

Mahler, H. C., Friess, W., Grauschopf, U., & Kiese, S. (2009). Protein aggregation: Pathways, induction factors and analysis. *Journal of Pharmaceutical Sciences, 98*(9), 2909–2934. https://doi.org/10.1002/jps.21566

Manouchehri, H. R., Rao, K. H., & Forssberg, K. S. E. (2000). Review of electrical separation methods - Part 1: Fundamental aspects. *Minerals and Metallurgical Processing, 17*(1), 23–36. https://doi.org/10.1007/BF03402825

Meighan, M. M., Keebaugh, M. W., Quihuis, A. M., Kenyon, S. M., & Hayes, M. A. (2009). Electrophoretic exclusion for the selective transport of small molecules. *Electrophoresis, 30*(21), 3786–3792. https://doi.org/10.1002/elps.200900340

Moshtarikhah, S., Oppers, N. A. W., de Groot, M. T., Keurentjes, J. T. F., Schouten, J. C., & van der Schaaf, J. (2017). Nernst–Planck modeling of multicomponent ion transport in a Nafion membrane at high current density. *Journal of Applied Electrochemistry, 47*(1), 51–62. https://doi.org/10.1007/s10800-016-1017-2

Najjar, Y. S. H., & Abu-Shamleh, A. (2020). Harvesting of microalgae by centrifugation for biodiesel production: A review. *Algal Research, 51*. https://doi.org/10.1016/j.algal.2020.102046

Nikiforidis, C. V. (2019). Structure and functions of oleosomes (oil bodies). *Advances in Colloid and Interface Science, 274*. https://doi.org/10.1016/j.cis.2019.102039

Nikiforidis, C. V., & Kiosseoglou, V. (2009). Aqueous extraction of oil bodies from maize germ (Zea mays) and characterization of the resulting natural oil-in-water emulsion.

Journal of Agricultural and Food Chemistry, 57(12), 5591–5596. https://doi.org/10.1021/jf900771v

Ntone, E., Bitter, J. H., & Nikiforidis, C. V. (2020). Not sequentially but simultaneously: Facile extraction of proteins and oleosomes from oilseeds. *Food Hydrocolloids, 102*. https://doi.org/10.1016/j.foodhyd.2019.105598

Ntone, E., Wesel, T. Van, Sagis, L. M. C., Meinders, M., Bitter, J. H., & Nikiforidis, C. V. (2021). Adsorption of rapeseed proteins at oil/water interface. Janus-like napins dominate the interface. *Journal of Colloid and Interface Science, 583*, 459–469. https://doi.org/10.1016/j.jcis.2020.09.039

van Oss, C. J. (1975). The influence of the size and shape of molecules and particles on their electrophoretic mobility. *Separation and Purification Reviews, 4*(1). https://doi.org/10.1080/03602547508066038

Östbring, K., Nilsson, K., Ahlström, C., Fridolfsson, A., & Rayner, M. (2020). Emulsifying and anti-oxidative properties of proteins extracted from industrially cold-pressed rapeseed press-cake. *Foods, 9*(678). https://doi.org/10.3390/foods9050678

Romero-Guzmán, M. J., Jung, L., Kyriakopoulou, K., Boom, R. M., & Nikiforidis, C. V. (2020). Efficient single-step rapeseed oleosome extraction using twin-screw press. *Journal of Food Engineering, 276*. https://doi.org/10.1016/j.jfoodeng.2019.109890

Romero-Guzmán, M. J., Köllmann, N., Zhang, L., Boom, R. M., & Nikiforidis, C. V. (2020). Controlled oleosome extraction to produce a plant-based mayonnaise-like emulsion using solely rapeseed seeds. *LWT - Food Science and Technology, 123*. https://doi.org/10.1016/j.lwt.2020.109120

Romero-Guzmán, M. J., Petris, V., De Chirico, S., di Bari, V., Gray, D., Boom, R. M., & Nikiforidis, C. V. (2020). The effect of monovalent (Na+, K+) and divalent (Ca2+, Mg2+) cations on rapeseed oleosome (oil body) extraction and stability at pH 7. *Food Chemistry, 306*. https://doi.org/10.1016/j.foodchem.2019.125578

Romero-Guzmán, M. J., Vardaka, E., Boom, R. M., & Nikiforidis, C. V. (2020). Influence of soaking time on the mechanical properties of rapeseed and their effect on oleosome extraction. *Food and Bioproducts Processing, 121*, 230–237. https://doi.org/10.1016/j.fbp.2020.03.006

Rosenthal, A., Pyle, D. L., & Niranjan, K. (1996). Aqueous and enzymatic processes for edible oil extraction. *Enzyme and Microbial Technology, 19*(6), 402–420. https://doi.org/10.1016/S0141-0229(96)80004-F

Rudge, S. R., & Monnig, C. A. (2000). Electrophoresis techniques. *Separation and Purification Methods, 29*(1), 129–148. https://doi.org/10.1081/SPM-100100006

Salazar-Villanea, S., Bruininx, E. M. A. M., Gruppen, H., Hendriks, W. H., Carré, P., Quinsac, A., & van der Poel, A. F. B. (2016). Physical and chemical changes of rapeseed meal proteins during toasting and their effects on in vitro digestibility. *Journal of Animal Science and Biotechnology, 7*(1), 1–11. https://doi.org/10.1186/s40104-016-0120-x

Saucedo-espinosa, M. A., & Lapizco-encinas, B. H. (2016). Refinement of current monitoring methodology for electroosmotic flow assessment under low ionic strength conditions. *Biomicrofluidics, 10*, 1–15. https://doi.org/10.1063/1.4953183

Schneider, C. A., Rasband, W. S., & Eliceiri, K. W. (2012). HISTORICAL commentary NIH image to ImageJ: 25 years of image analysis. *Nature Methods, 9*(7), 671–675. https://doi.org/10.1038/nmeth.2089

Semenov, I., Papadopoulos, P., Stober, G., & Kremer, F. (2010). Ionic concentration- and pH-dependent electrophoretic mobility as studied by single colloid electrophoresis. *Journal of Physics: Condensed Matter, 22*, 1–5. https://doi.org/10.1088/0953-8984/22/49/494109

Tan, S. H., Mailer, R. J., Blanchard, C. L., & Agboola, S. O. (2011). Canola proteins for human consumption: Extraction, profile, and functional properties. *Journal of Food Science, 76*(1). https://doi.org/10.1111/j.1750-3841.2010.01930.x

Torres-Acosta, M. A., Mayolo-Deloisa, K., González-Valdez, J., & Rito-Palomares, M. (2019). Aqueous two-phase systems at large scale: Challenges and opportunities. *Biotechnology Journal, 14*(1). https://doi.org/10.1002/biot.201800117

USDA. (2022). Oilseeds: World markets and trade. July 2021, 1–38 https://downloads.usda.library.cornell.edu/usda-esmis/files/tx31qh68h/r781xd48h/4f16d011j/oilseeds.pdf.

Zhou, Y., Zhao, W., Lai, Y., Zhang, B., & Zhang, D. (2020). *Edible Plant Oil: Global Status, Health Issues, and Perspectives, 11*, 1–16. https://doi.org/10.3389/fpls.2020.01315